The influence of the magnetic field perturbation onto the divertor target deposition in W7-AS

F. Gadelmeier and J. Kißlinger

Max-Planck-Institut für Plasmaphysik, EURATOM Association, D-85748 Garching

1. Introduction

The main purpose of this paper is to validate the field line diffusion modelling used for the design of the W7-AS divertor, [1]. In this sense, the toroidal distribution of the strike points calculated by means of field line diffusion is compared to the energy deposited onto the divertor targets (target load). The experimental data show that the target load of several divertor modules changes significantly at $\iota_a \sim 0.5$, ι_a is the rotational transform at the edge. Considering the m = 2 perturbation of the magnetic field in the field line diffusion modelling, the toroidal strike point distribution coincides fairly well with the measured target load. Further, the paper shows the influence of the m = 2 perturbation on the shape of the magnetic flux surfaces.
In the present study low β-discharges with a line integrated density of 10^{19} m^{-3}, 850 kW ECRH and B_t = -2.5 T are employed. ι_a ranges from 0.472 to 0.573; in the range of 0.492 to 0.573 ι_a varies in steps of ~0.005. The distribution of the target load in toroidal direction is shown in figure 1. White spaces mark divertor regions where no information about the deposited energy is available. The arrangement of the divertor modules is given in figure 2. A clear change of the target load at $\iota_a \sim 0.5$ is evident; towards higher ι_a the maximums at the upper modules 2 and 4 disappear and new maximums arise at the upper and lower module 1. The toroidal and up/down asymmetries of the target load at fixed ι_a are mainly due to vertical displacements of the divertor modules relative to a symmetric arrangement. They are determined from experimental target load data and taken into account in the field line diffusion modelling. In section 2 the vertical displacements of the divertor modules are determined. Section 3 deals with the m = 2 perturbation.

2. Determination of the divertor module displacements

In a limiter discharge the divertor module closest to the plasma defines the plasma edge. All the other modules are exposed to an energy flux, *Q*, that decays exponentially with a decay length, λ. The total energy deposited at a divertor module is calculated using the field line diffusion modelling for various vertical positions of the ten divertor modules and various diffusion coefficients *D*. In order to determine the real position of the divertor modules the quantity that has to be minimized in this variation problem is: $Q_{modelled} - Q_{measured}$. Since the

vertical positions of the divertor modules, z_i, $i = 1\ldots10$, are related to $Q(z_i) = constant \times exp(z_i/\lambda)$, the ten dimensional variation problem reduces to a two dimensional one with the independent variables λ and D.

Figure 3 shows target load profiles measured in two limiter discharges at $\iota_a = 0.396$ and $\iota_a = 0.445$, respectively. The energy flux is maximum at the upper module #4 and decreases continuously at the upper modules #5, #2, #3, #1, the lower modules #1, #5, #4, #3, and #2. Apart from minor differences this order is the same for both magnetic configurations. Applying the least square method to the variation problem described above, the target load profiles given in figure 3 deliver a decay length of 7 to 8 mm and a diffusion coefficient of 2 to 3 m^2/s. The resulting vertical displacements of the divertor modules relative to a symmetric arrangement are shown in table 1. In the field line diffusion modelling the average values given in column 4 of table 1 and $D = 2\ m^2/s$ are used.

3. The m = 2 perturbation and their influence on target load and magnetic flux surfaces

The existence of a m = 2 perturbation in the magnetic field of W7-AS is demonstrated in [2]. Figure 4 shows flux surface cross-sections in the triangular plane measured with the fluorescent rod technique in a magnetic configuration where $\iota_a = 0.503$, [2]. At the edge, two m = 2 islands are clearly evident; each of them encloses five m = 10 islands. Using a field line tracing technique, a homogenous horizontal error field of 5×10^{-4} is deduced from figure 4. According to the perturbation field spectrum given in [2], this error field produces a B_{22} Fourier component of approximately 7×10^{-5}.

In order to study the influence of the m = 2 perturbation on the target wetting, field line diffusion modelling is employed. The number of strike points per divertor module is calculated for all magnetic configurations given in section 1. It is assumed, that the modelling obeys the Poisson statistic. The statistical error amounts 3 to 6 %.

First, the field line diffusion modelling is done without the m = 2 perturbation. The resulting toroidal strike point distributions show no relocation of the maximum with ι_a. This is clear evidence that the redistribution of the target load at $\iota_a \sim 0.5$ in figure 1 is not due to the inaccurate adjustment of the divertor modules. Secondly, the m = 2 perturbation is included in the field line diffusion modelling and the resulting toroidal strike point distribution is compared to the energy deposition profile determined experimentally[1]. The absolute value of the error field is assumed to be constant, equal to 11.2×10^{-4} T. Its x and y components, B_x *and* B_y, are varied so that the field line diffusion modelling reflects the experimentally observed

[1] The upper divertor modules #3 and #5 as well as the lower modules #2 and #4 are excluded from this comparison, since there is only little information about their target load available. Further, the energy deposited onto the 17 tiles of a module is summed up, so that it can be compared to the number of strike points per module. The new, but equivalent representation of figure 1 is shown in figure 5.

relocation of the maximum target load. The z component, B_z, is set to zero, since it does not affect the m = 2 perturbation.

The right hand side of figure 6 shows the toroidal strike point distribution versus ι_a calculated for two different sets of B_x and B_y. The left hand side of figure 6 represents the corresponding flux surface cross-sections at the toroidal positions φ = 216°, 252° and 324° in the case of ι_a = 0.503. The appearance of two m = 2 islands at the edge is evident. The position of these islands in poloidal direction (the phase of the island) depends on B_x and B_y. Since the phase of the island varies in toroidal direction, the m = 2 perturbation leads to an asymmetric ι-dependent strike point distribution, as demonstrated in figure 6. The upper strike point distributions of figure 6 does not reflect the redistribution of the target load observed in figure 5, e.g. the number of strike points at the upper module 2 increases at $\iota \sim 0.51$, whereas the target load at the same module decreases. In the case of the lower strike point distributions of figure 6, the ι-dependence at each module shows the same features as the target load in figure 5. However, the absolute values does not agree, e.g. at $\iota > 0.53$ the number of strike points is maximum at the upper module 2, whereas the target load at the same module nearly vanishes. This discrepancy is mainly due to an inaccurate knowledge of the divertor module displacements. The sensitivity of the strike point distribution on the vertical displacements of the divertor modules is demonstrated in figure 7 where the vertical position is readjusted. It shows, that an appropriate slightly change (within the error bars) of the displacements leads to a convergence of the absolute values. A further improvement can be expected by changing the diffusion coefficient within the error bars. Apart from the remaining differences, the field line diffusion modelling predicts the redistribution of the target load at $\iota_a \sim 0.5$, provided that appropriate B_x and B_y components of the error field are chosen. Once validated, the method described above also allows for an estimation of the error field.

The deformation of the magnetic flux surfaces due to the m = 2 perturbation is illustrated in the figures 8 and 9. In figure 8 flux surface cross-sections of a m = 2 perturbed magnetic configuration are compared to an ideal one. Although the m = 2 islands are no more present in the configuration ($\iota > 0.5, \forall r < a$) the deformation of the central flux surfaces at ι_a = 0.516 remains remarkable. The maximum deviation from the ideal flux surfaces in the triangular plane φ = 216° amounts up to 2 cm. The deformation reduces with the distance of ι_a to 0.5, e.g. at ι_a = 0.527 the flux surfaces coincide. Figure 9 shows the deformation of the outer flux surface cross-sections in a magnetic configuration with ι_a = 0.527. This can easily be seen comparing the distances of the last shown flux surface to the divertor targets. In an unperturbed configuration with symmetrically arranged divertor targets this distance does not vary. In figure 9, however, it depends on the toroidal position; the distance to the lower target #3 amounts up to 15 mm, and only 2 ... 4 mm to the lower targets #1 and #5. Since this variation is comparable to the decay length of the energy flux at the plasma edge, a significant influence of the error field on the target load may be expected. According to figure 1, this influence does not restrict only to magnetic configurations with m = 2 islands included, i.e. $\iota_a \sim 0.5$, but also on configurations with ι_a lower and beyond 0.5.

4. Conclusions

Assuming a relative homogenous horizontal field perturbation of 5×10^{-4} with appropriate B_x and B_y components, the field line diffusion modelling predicts the relocation of the maximum energy deposition observed at $\iota_a \sim 0.5$. Field line tracing shows that the perturbation leads to a considerable distortion of the flux surfaces, especially in magnetic configurations with $\iota_a \sim 0.5$. In this case, both, the central and the edge flux surfaces are affected. The distortion reduces with the distance of ι_a to 0.5. Nevertheless, even at $\iota_a = 0.527$ it is strong enough to affect the energy deposition at the divertor targets.

In general, the present study reveals that a sufficient large error field changes the energy deposition onto the divertor targets leading to toroidal and up/down asymmetries. It also shows, that the field line diffusion modelling is a reliable tool to determine the permissible limits of the error fields, and thus the accuracy of the coil fabrication, machine assembly, etc. Further, the deformation of the flux surfaces due to large resonant Fourier components complicates the mapping of profiles measured at different toroidal positions. In this case, the knowledge of the resonant Fourier components is obligatory.

By the way, a simple technique has been developed to determine the displacements of the divertor modules relative to a symmetric arrangement.

References

[1] J. Kisslinger et al., Proc. 22th EPS Conf. on Contr. Fus. Plasma Phys. (Bournemouth), vol. 19C, part III, (1995) 149

[2] R. Jaenicke, E. Ascasibar, P. Grigull et al., Nuclear Fusion, Vol.33, No.5 (1993), 687-704

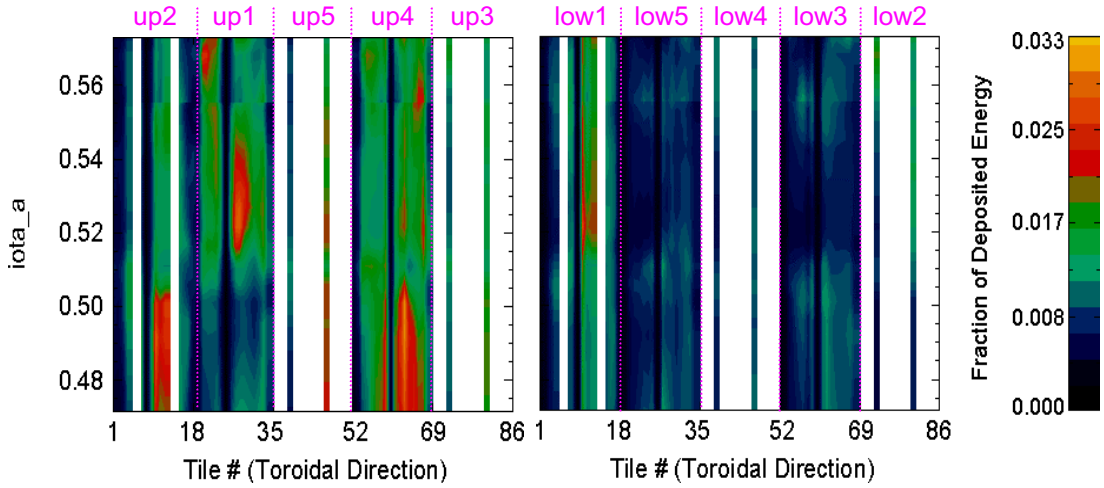

Figure 1: Energy deposited onto the divertor targets versus ι_a; dashed lines separate individual modules; each module consists of 17 target plates

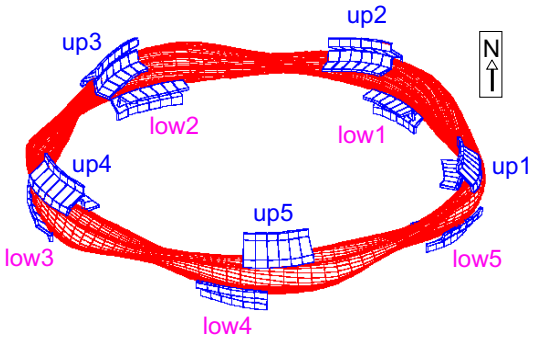

Figure 2: Divertor module arrangement at W7-AS

Divertor Module	Δz [cm] at ι=0.396	Δz [cm] at ι=0.445	Δz [cm] (average)	Δz [cm] (adjusted)
lower2	0.45	0.49	0.47	0.49
lower3	0.43	0.33	0.38	0.38
lower4	0.36	0.26	0.31	0.31
lower5	0.25	0.17	0.21	0.25
lower1	0.08	0.11	0.09	0.09
upper1	-0.21	0.06	-0.07	-0.21
upper3	-0.41	-0.29	-0.35	-0.29
upper2	-0.44	-0.26	-0.35	-0.20
upper5	-0.52	-0.40	-0.46	-0.51
upper4	-0.52	-0.52	-0.52	-0.70

Table I: Displacements Δz of the divertor modules relative to a symmetric arrangement; Δz in the 5th column are slightly modified from an exponential decay

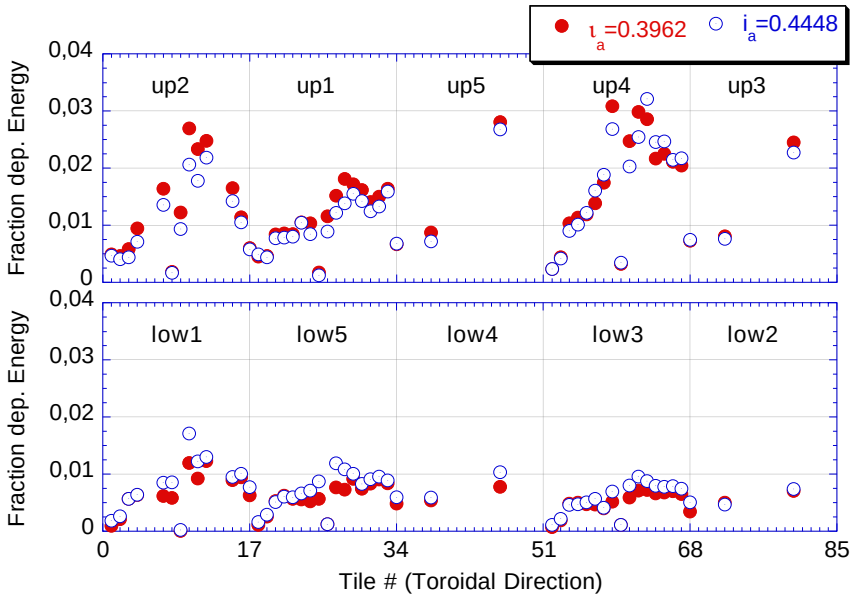

Figure 3: Energy deposition profiles at the targets in limiter discharges (#50440 and #50443)

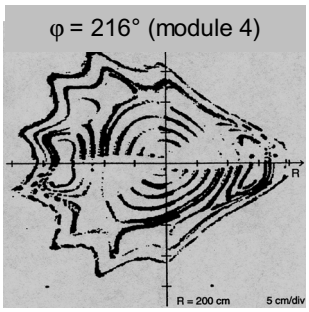

Figure 4: Measured flux surface cross-section for ι_a=1/2, [2]; each m = 2 island encloses five islands due to ι_a = 5/10

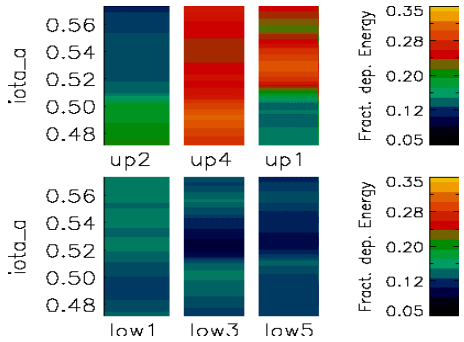

Figure 5: The energy (sum over 17 tiles) deposited onto the six divertor modules versus ι_a or target load profile (abbreviated)

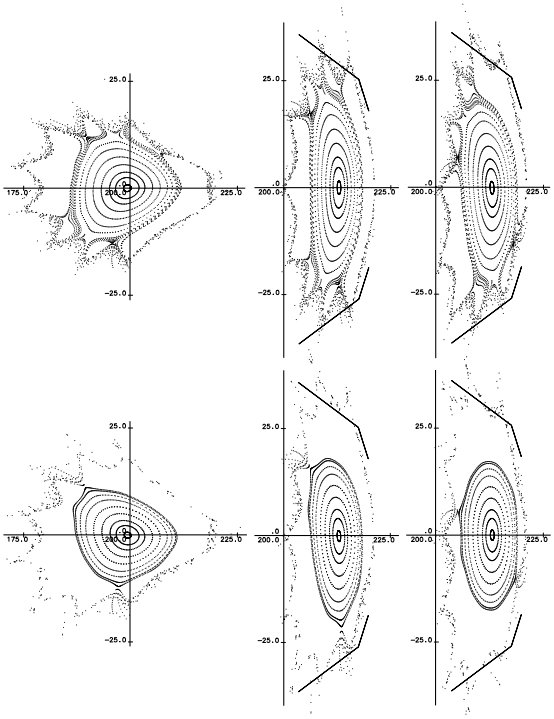

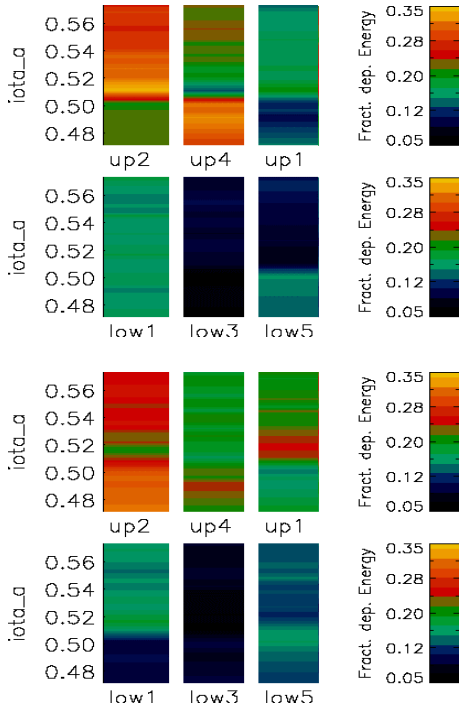

Figure 6: Calculated strike point distributions versus ι_a at the perturbations: B_x= 10 G, B_y= -5 G (upper) and B_x= -2.7 G, B_y= -10.8 G (lower); and coressponding flux surface cross-sections of a ι_a=0.503 configuration at φ = 216° and 252° (module 4) and φ = 324° (module 5); the target wetting of the modules is not symmetric due to the different island phases

Figure 7:
Calculated strike point distribution versus ι_a at the perturbation B_x= -2.7 G, B_y= -10.8 G using the vertical displacements given in the 5th column of table I

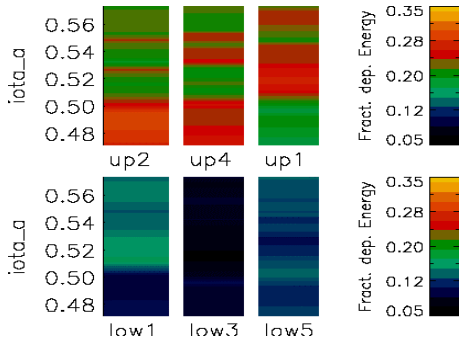

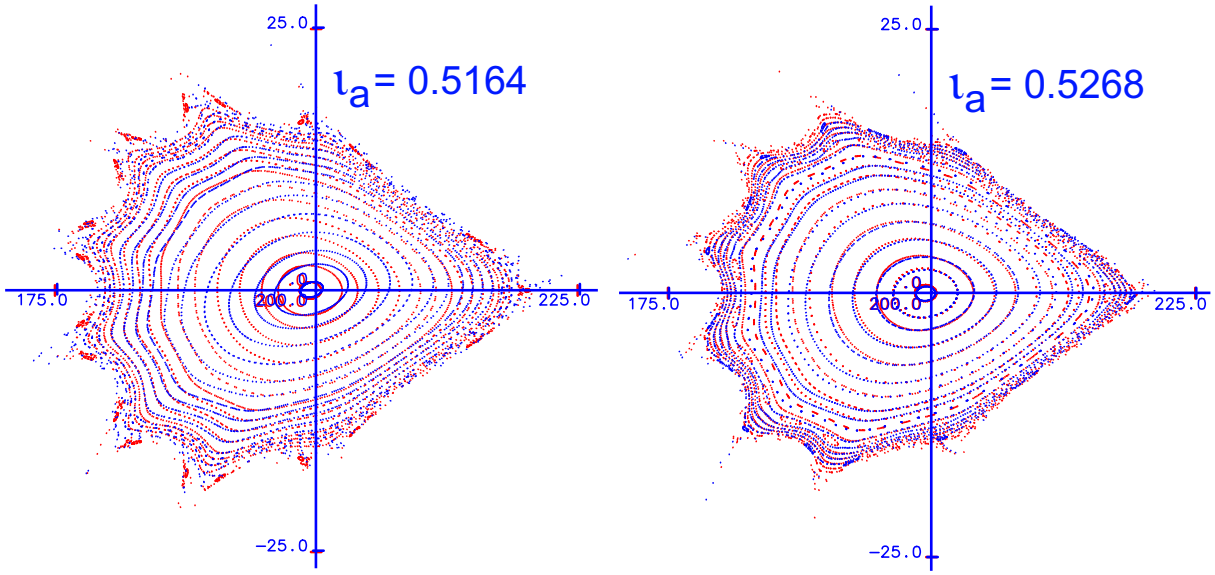

Figure 8: Flux surface cross-sections at φ = 216° (module 4) without (red) and with the perturbation (blue): B_x = -5 G, B_y = -10 G; the scale unit is cm

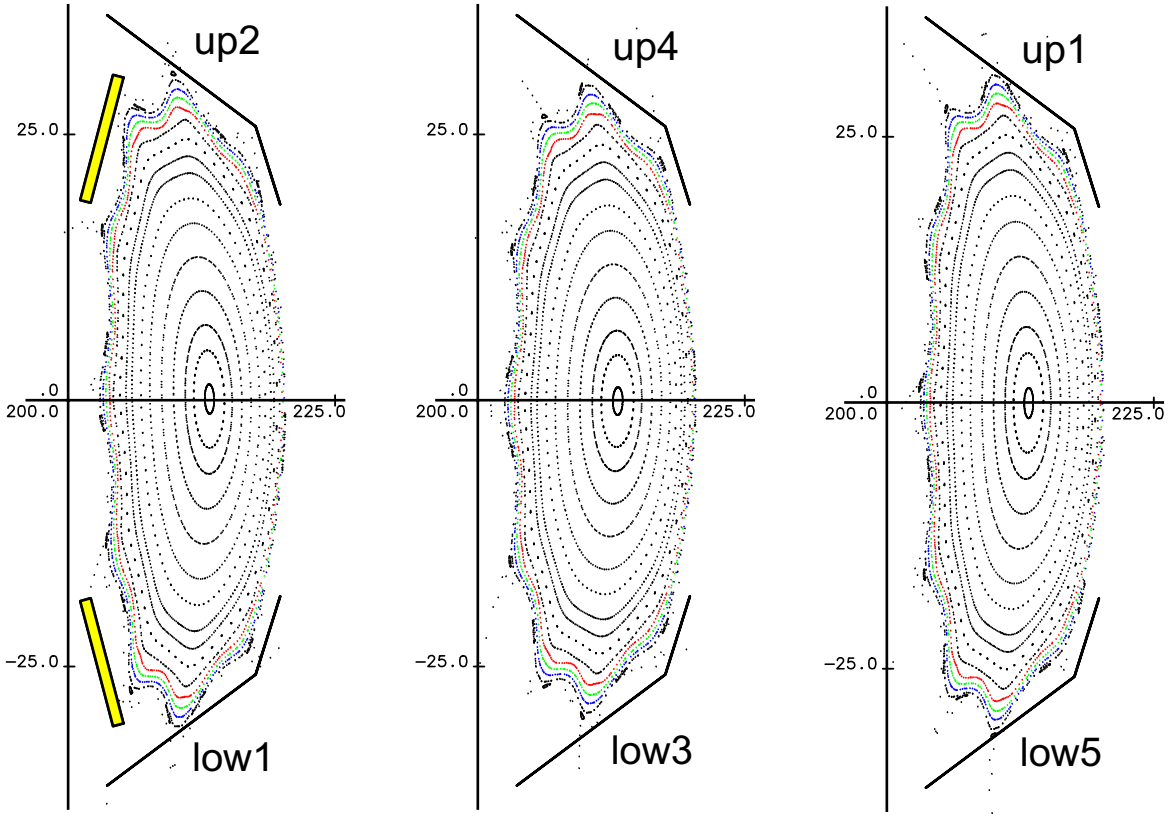

Figure 9: Flux surface cross-sections at ι_a=0.527 in the elliptical planes φ = 36°, 180° and 324° calculated in the presence of the perturbation: B_x = -5G, B_y = -10G; the divertor modules are symmetrically arranged in the model; the scale unit is cm